BER Performance of Turbo-Coded PPM CDMA Systems on Optical Fiber

Tomoaki Ohtsuki, *Member, IEEE,* and Joseph M. Kahn, *Fellow, IEEE*

***Abstract*—We obtain upper bounds on the bit error rate (BER) for turbo-coded optical code-division multiple-access (CDMA) systems using pulse position modulation (PPM). We use transfer function bounding techniques to obtain these bounds, so our results correspond to the average bound over all interleavers of a given length. We consider parallel concatenated coding (PCC) schemes that use recursive convolutional codes as constituent codes. We consider systems using an avalanche photodiode (APD), and treat APD noise, thermal noise, and multi-user interference using a Gaussian approximation. We compare the performance of turbo-coded systems with that of BCH-coded systems with soft-decision decoding, and that of concatenated coding systems with outer Reed-Solomon (RS) code and inner convolutional code. We show that turbo-coded systems have better performance than BCH-coded systems. We also show that concatenated systems have better performance than turbo-coded systems when the block length is small and the received laser power is somewhat large.**

***Index Terms*—Optical code division multiple access (CDMA), pulse position modulation (PPM), turbo codes.**

I. Introduction

RECENTLY, optical code-division multiple-access (CDMA) schemes have attracted much attention particularly in the field of fiber-optic networks, because they allow multiple users to access the network asynchronously and simultaneously [1]–[6]. Optical CDMA is advantageous in that it makes channel assignment easier than in time-division multiple-access (TDMA) or frequency-division multiple-access (FDMA) systems. Thus, optical CDMA is an attractive option for future optical access networks.

In optical CDMA systems, multi-user interference is one of the most serious problems. To improve performance of optical CDMA systems in the presence of multi-user interference, some researchers have applied error-correction codes, such as convolutional codes, Reed-Solomon (RS) codes, and BCH codes [3], [4].

Recently, turbo codes have attracted much attention because of their astonishing error performance and their reasonable decoding complexity [7]–[10]. Fig. 1(a) and (b) show the structures of turbo code and turbo decoder. Turbo codes are parallel concatenated convolutional codes (PCCCs) whose encoder comprises identical recursive convolutional encoders that are preceded by different interleavers, and whose output bits are concatenated in parallel. A turbo decoder consists of the corresponding decoders with a de-interleaver in between to modify error patterns in the received sequence, and employs iterative decoding. The output of each component decoder contains three terms: systematic information generated by the code information bit, extrinsic information generated by the code parity check bit, and a priori information generated by the other decoder. The extrinsic information is exchanged between the two component decoders. It was confirmed by computer simulation that by increasing the number of iterations a bit error rate (BER) of 10^{-4} can be obtained at an information bit signal-to-noise ratio (SNR) E_b/N_0 as low as -0.15 dB [11].

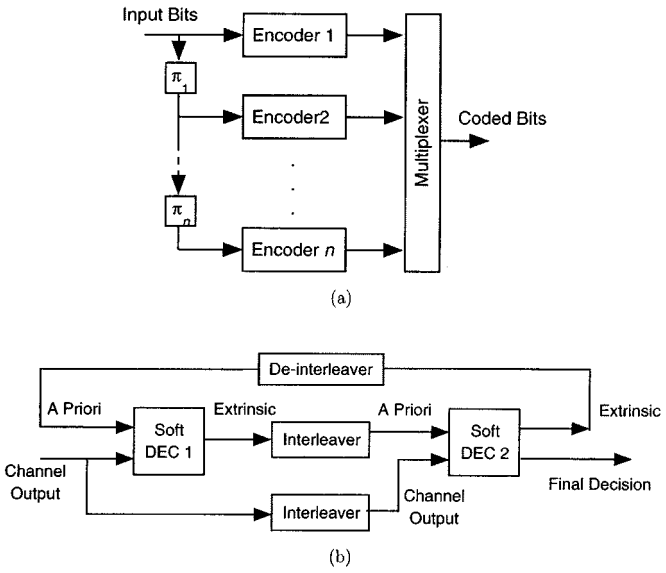

Fig. 1. Structures of turbo encoder and turbo decoder: (a) turbo code structure and (b) turbo decoder structure.

In addition to computer simulations, it is also very useful to have theoretical bounds in the range where the computer simulations is not feasible. Some researchers have developed the very useful transfer function technique to obtain upper bounds on the BER for maximum-likelihood (ML) decoding of turbo codes for binary orthogonal signals [8]–[10]. As for convolutional codes, the error probability is upper-bounded by a union bound that sums contributions from error paths of different encoded weights, and the state diagram of the code is used to enumerate the paths of each possible weight. However, there are some differences between the transfer-function bounds for turbo codes and those for convolutional codes [8]. First, the bounds for turbo codes require a joint enumerator for all possible combinations of input weights and output weights of error events.

Manuscript received April 5, 2000; revised September 19, 2000. This work was supported in part by the Mazda Foundation and the Okawa Foundation for Information and Telecommunications.

T. Ohtsuki is with the Department of Electrical Engineering, Science University of Tokyo, Noda 278–8510, Japan; (e-mail: ohtsuki@ee.noda.sut.ac.jp).

J. M. Kahn is with the Department of Electrical Engineering and Computer Sciences, University of California, Berkeley, CA 94720 USA.

Publisher Item Identifier S 0733-8724(00)10996-X.

Second, since turbo codes are block codes, it is difficult to enumerate compound error events that include more than one excursion from the all-zero state within the fixed block length. Third, since it is difficult to obtain the bound for any particular choice of permutation, the bound is developed as an average over randomly chosen interleavers. Reference [12] applied the above transfer function bounding techniques to turbo-coded optical binary PPM (BPPM) systems. It was shown in [12] that turbo codes can provide substantial coding gain with a reasonable system complexity for optical PPM systems. However, performance of turbo-coded optical PPM CDMA systems has not been clarified.

In this paper, we obtain upper bounds on the BER for turbo-coded optical CDMA systems using pulse position modulation (PPM). We use transfer function bounding techniques to obtain these bounds, so our results correspond to the average bound over all interleavers of a given length. Note that since the transfer function bound is developed for the ML decoding, we cannot say the number of iterations of turbo decoding. We consider parallel concatenated coding (PCC) schemes that use recursive convolutional codes as constituent codes. We consider systems using an avalanche photodiode (APD), and treat APD noise, thermal noise, and multi-user interference using a Gaussian approximation. We compare the performance of turbo-coded optical PPM CDMA systems with that of BCH-coded optical PPM CDMA systems with soft-decision decoding [13], [14], and that of concatenated coding systems with outer RS code and inner convolutional code. We show that turbo-coded optical CDMA systems have better performance than BCH-coded optical PPM CDMA systems. We also show that concatenated systems have better performance than turbo-coded systems when the block length is small and the received laser power is somewhat large.

II. System Model

Direct-detection optical CDMA systems require $\{0,1\}$-valued code sequences with good correlation properties: small cross-correlations between the sequences are essential for low multi-user interference. As our signature code sequences, we employ low-weight Optical Orthogonal Codes (OOCs) with out-of-phase auto-correlations and cross-correlations bounded by one. We assume each user to be assigned an optical code sequence of OOCs with length F and weight K. The correlation characteristics of OOCs are represented by [15]

$$|C_{a^x,a^x}(l)| = \left|\sum_{i=0}^{F-1} a_i^x a_{i+l}^x\right| = \begin{cases} K, & \text{for } l=0, \\ \le \Lambda_a = 1, & \text{for } 1 \le l \le F-1, \end{cases} \quad (1)$$

$$|C_{a^x,a^y}(l)| = \left|\sum_{i=0}^{F-1} a_i^x a_{i+l}^y\right| \le \Lambda_c = 1, \quad \text{for } 0 \le l \le F-1. \quad (2)$$

where a^x and a^y represent sequences of OOCs. For OOC with length F, weight K, and the maximum values of out-of-phase-auto- and cross-correlations equal to one, the number of code sequences is upper bounded by $N \le \lfloor (F-1)/K(K-1) \rfloor$.

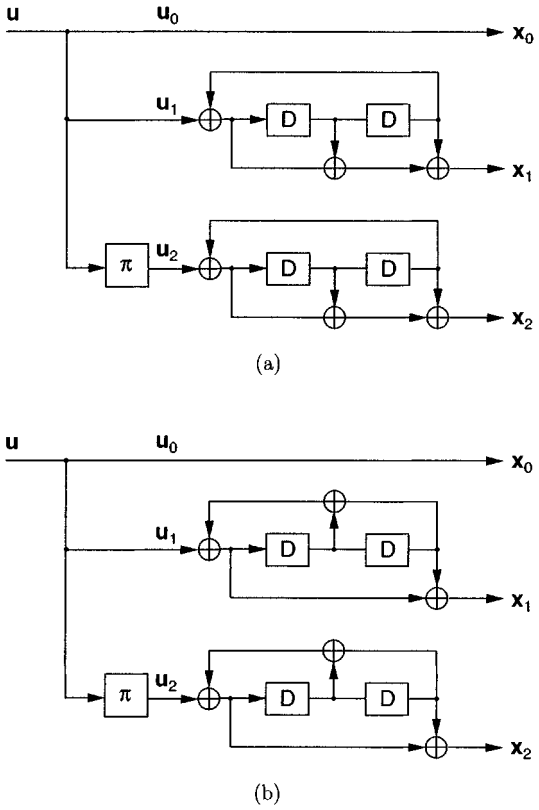

Fig. 2. Two typical turbo encoders: (a) the $(1, 7/5, 7/5)$ code and (b) the $(1, 5/7, 5/7)$ code.

Figs. 2(a) and 1(b) show the encoders for the two turbo codes under study. Note that turbo-coding and turbo-decoding in our system are done in the electrical domain. As the encoders employ parallel concatenation of constituent convolutional codes, the codes are often called parallel concatenated convolutional codes (PCCCs). Both encoders produce one uncoded output stream $\mathbf{x_0}$ and two encoded parity output streams $\mathbf{x_1}$ and $\mathbf{x_2}$. Thus, the code rates of both codes are $1/3$. The parity streams in these encoders come from the simple recursive convolutional encoders with constraint length $\nu = 3$. For the codes in Fig. 2(a), both parity sequences correspond to a ratio of generator polynomials g_a/g_b where $g_a(D) = 1+D+D^2$ and $g_b(D) = 1+D^2$. For the codes in Fig. 2(b), both parity sequences correspond to a ratio of generator polynomials g_b/g_a. In octal, the two codes are denoted by $(1, 7/5, 7/5)$ and $(1, 5/7, 5/7)$, respectively. The three separate rate-1 components of the code are referred to as code fragments. Thus, a turbo code can be viewed as a parallel concatenation of some code fragments, and the parallel concatenation forms the full codeword. Any codeword of turbo code has the following structure:

$$(\mathbf{i}|\psi(\mathbf{i})|\psi(\pi(\mathbf{i}))) \quad (3)$$

where

- $\mathbf{i}$ N_I-tuple of the information bits,;
- $\pi(\mathbf{i})$ version of $\mathbf{i}$ with interleaved (permutated) coordinates;
- $\psi(\cdot)$ map from the information bits to the parity check bits generated by the component encoder.

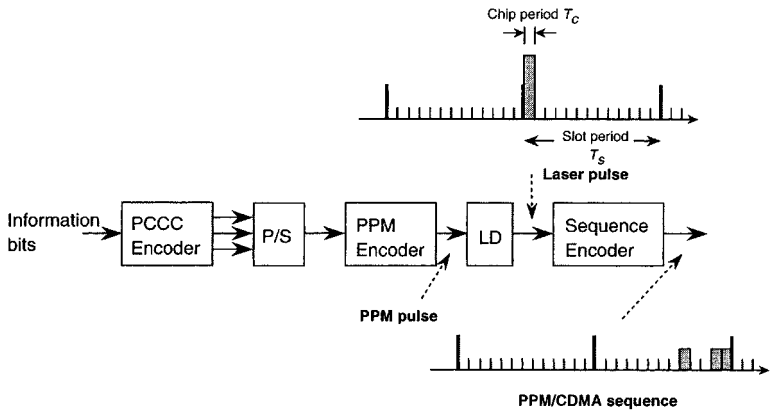

Fig. 3. Transmitter block diagram of turbo-coded optical PPM CDMA system.

To analyze the performance of turbo codes theoretically, we want to know, for a given interleaver, the input-output weight enumerator function (IOWEF), sometimes called the input-redundancy weight enumerating function (IRWEF). However, to obtain the IOWEF for a given interleaver is exceedingly complicated, because the redundant bits generated by the second constituent encoder will depend not only on the weight of the input word, but also on the permutation preceding the encoder. To overcome this difficulty, we introduce a random interleaver, sometimes called a uniform interleaver [8], [9]. A random interleaver of length N_I is a probabilistic device that maps a given input word of weight d into one of its $\binom{N_I}{d}$ distinct permutations, each with equal probability $1/\binom{N_I}{d}$. Each of the encoders in Fig. 2(a) and (b) is used to generate a $(3(N_I+2), N_I)$ block code, where N_I is the information block length. Following the information bits, an additional two "tail bits" are appended to initialize the encoder, that is, to drive the encoder to the all-zero state at the end of the block. Here, we use the termination method described in [16]. Since the component encoders are recursive, it is impossible to terminate both component encoders with the same m bits. Usually only the first encoder is forced to to return to the initial state by appending tail bits [17]. Note that the performance degradation caused by the ambiguity of the final state of the second encoder is negligible for a large N_I [18].

Fig. 3 shows the transmitter block diagram of the turbo-coded optical PPM CDMA system. We consider binary PPM (BPPM) to apply the transfer function bounding technique to PPM. Thus, a single coded bit is mapped to each BPPM symbol. A laser pulse is emitted on the 0th or first slot according to a coded bit. Fig. 4 shows the sequence encoder comprising a set of optical fiber delay lines. The output laser pulse is converted into the assigned optical code sequence, that is, the signature code sequence by the sequence encoder comprising a set of optical fiber delay lines. Then, the pulses spread over the slot are transmitted over the fiber to the desired destination. Fig. 5 shows the receiver block diagram of turbo-coded optical PPM CDMA system. The received signal is first put into the optical correlator shown in Fig. 6. The optical correlator is a set of optical delay lines inversely matched to the pulse spacings. The optical intensity received at the positions of "1" of the code sequence for

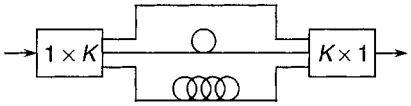

Fig. 4. Sequence encoder comprising a set of optical fiber-delay lines.

the desired channel is summed up at the last chip. The output of the optical correlator is converted into the electrical signal by the APD. Note that we use the incoherent matched filtering technique not the coherent matched filtering technique. For the latest demonstration work on the incoherent matched filtering, see [19].

For turbo codes, a practical decoding algorithm was presented in [7]. The algorithm is referred to as the iterative decoding algorithm. Suppose $\mathbf{x} = (\mathbf{u}, \psi(\mathbf{u}), \psi(\pi(\mathbf{u})))$ is the codeword corresponding to the information sequence $\mathbf{u} = (u_1, u_2, \ldots, u_{N_I})$ and $\mathbf{y} = (\mathbf{y_0}, \mathbf{y_1}, \mathbf{y_2})$ is the noise corrupted version of $\mathbf{x}$. The optimal decision algorithm on the ith information bit u_i is based on the ratio of a posteriori probabilities

$$L_i^{(\mathrm{opt})} = \frac{P(u_i = 1 \,|\, \mathbf{y})}{P(u_i = 0 \,|\, \mathbf{y})}, \quad i = 1, 2, \ldots, N_I. \tag{4}$$

If $L_i^{(\mathrm{opt})} \geq 1$, the decoder estimates that $u_i = 1$, otherwise $u_i = 0$. Let define $F_i(u)$ as $F_i(u) = \{\mathbf{u} \in \mathbf{F}^{N_I}; u_i = u\}$ for $i = 1, 2, \ldots, N_I$ and $u \in \mathbf{F} = \{0, 1\}$. Assuming equiprobable inputs, (4) can be written as

$$L_i^{(\mathrm{opt})} = \frac{\sum_{\mathbf{u} \in F_i(1)} P\left(\mathbf{y}^{(1)} \,\middle|\, \mathbf{x}^{(1)}\right) P\left(\mathbf{y}^{(2)} \,\middle|\, \mathbf{x}^{(2)}\right)}{\sum_{\mathbf{u} \in F_i(0)} P\left(\mathbf{y}^{(1)} \,\middle|\, \mathbf{x}^{(1)}\right) P\left(\mathbf{y}^{(2)} \,\middle|\, \mathbf{x}^{(2)}\right)} \tag{5}$$

where $\mathbf{x}^{(1)} = (\mathbf{u}, \psi(\mathbf{u}))$, $\mathbf{x}^{(2)} = (\pi(\mathbf{u}), \psi(\pi(\mathbf{u})))$, $\mathbf{y}^{(1)} = (\mathbf{y}_0, \mathbf{y}_1)$, and $\mathbf{y}^{(2)} = (\pi(\mathbf{y}_0), \mathbf{y}_2)$. Although the optimal decoding can be done by computing the $L_i^{(\mathrm{opt})}$'s, it is difficult to compute them.

The iterative decoding algorithm computes $L_i^{(k)}$'s for $k = 1, 2, \ldots$. In the iterative decoding algorithm, the results of component decoders are exchanged through the feedforward and the

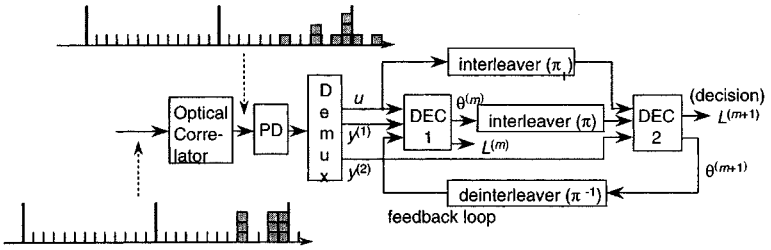

Fig. 5. Receiver block diagram of turbo-coded optical PPM CDMA system.

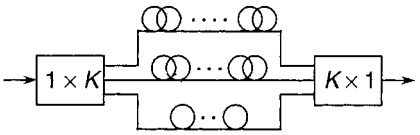

Fig. 6. Optical correlator comprising a set of optical fiber-delay lines.

feedback loop. The decoder 1 in Fig. 3 computes the following likelihood ratios for the u_i's based on $\mathbf{y}^{(1)}$

$$L_i = \frac{\sum_{\mathbf{u}\in F_i(1)} P\left(\mathbf{y}^{(1)} \mid \mathbf{x}^{(1)}\right) \prod_{j=1}^{N_I} p_j(u_j)}{\sum_{\mathbf{u}\in F_i(0)} P\left(\mathbf{y}^{(1)} \mid \mathbf{x}^{(1)}\right) \prod_{j=1}^{N_I} p_j(u_j)} \tag{6}$$

where $p_j(u_j)$'s are provided by the Decoder 2. Similarly, the Decoder 2 computes likelihood ratios for the u_i's based on $\mathbf{y}^{(2)}$ and $p_j(u_j)$'s which are provided by the Decoder 1. Letting $p_j(u_j)$ denote the a priori probabilities, (6) can be written as

$$L_i = \frac{P\left(u_i = 1 \mid \mathbf{y}^{(1)}\right)}{P\left(u_i = 0 \mid \mathbf{y}^{(1)}\right)}. \tag{7}$$

For $k = 1, 2, \ldots$ and $i = 1, 2, \ldots, N_I$, let $L_i^{(k)}$ and $\theta_i^{(k)}$ be defined as (8) and (9), shown at the bottom of the page, where

$p_j^{(k-1)}(0) = 1/(1+\theta_j^{(k-1)})$,
$p_j^{(k-1)}(1) = \theta_j^{(k-1)}/(1+\theta_j^{(k-1)})$,
$\theta_j^{(0)} = 1$ for all j

Using the above equations, the iterative decoding algorithm for Turbo codes can be implemented.

III. Union Bounds on Word- and Bit-Error Probabilities

We analyze performance of turbo-coded optical PPM CDMA system by using the Gaussian approximation of the APD output [20], [21]; the effects of APD noise, thermal noise, and multi-user interference are considered. The primary reason for using APDs with internal gains, as opposed to PIN diodes with constant unity gain, is that they have larger responsivity and are more sensitive to the incoming photons. APDs are preferable to PIN diodes when the system is thermal-noise-limited, as opposed to shot-noise-limited. The performance is analyzed in the chip-synchronous case and thus the performance results in the upper bounds on that of the system.

The probability that a specified number of photons are absorbed from an incident optical field by an APD detector over a chip interval with T_c is given by a Poisson distribution. The average number of absorbed photons over T_c is $\lambda_s T_c$ where λ_s is the photon absorption rate written as

$$\lambda_s = \frac{\eta P_W}{hf} \tag{10}$$

where

P_W laser power;
η APD efficiency with which the APD converts incident photons to photoelectrons;
h Plank's constant;
f optical frequency.

Primary photoelectron-hole pairs in the APD detector undergo an avalanche multiplication process that results in the output of m_e electrons from the APD in response to the absorption of λT_c primary photons on the average: λ represents the total photon absorption rate due to signal, background, and APD bulk leakage current

$$\lambda = \begin{cases} \lambda_s + \lambda_b + I_b/e, & \text{for ``1''} \\ \lambda_s/M_e + \lambda_b + I_b/e, & \text{for ``0''} \end{cases} \tag{11}$$

$$L_i^{(k)} = \begin{cases} \dfrac{\sum_{\mathbf{u}\in F_i(1)} P\left(\mathbf{y}^{(1)} \mid \mathbf{x}^{(1)}\right) \prod_{j=1}^{N_I} p_j^{(k-1)}(u_j)}{\sum_{\mathbf{u}\in F_i(0)} P\left(\mathbf{y}^{(1)} \mid \mathbf{x}^{(1)}\right) \prod_{j=1}^{N_I} p_j^{(k-1)}(u_j)}, & \text{if } k \text{ is odd,} \\ \dfrac{\sum_{\mathbf{u}\in F_i(1)} P\left(\mathbf{y}^{(2)} \mid \mathbf{x}^{(2)}\right) \prod_{j=1}^{N_I} p_j^{(k-1)}(u_j)}{\sum_{\mathbf{u}\in F_i(0)} P\left(\mathbf{y}^{(2)} \mid \mathbf{x}^{(2)}\right) \prod_{j=1}^{N_I} p_j^{(k-1)}(u_j)}, & \text{if } k \text{ is even,} \end{cases} \tag{8}$$

$$\theta_i^{(k)} = \begin{cases} L_i^{(k)} \Big/ \theta_{\pi(i)}^{(k-1)}, & \text{if } k \text{ is odd,} \\ L_i^{(k)} \Big/ \theta_{\pi^{-1}(i)}^{(k-1)}, & \text{if } k \text{ is even,} \end{cases} \tag{9}$$

where

- λ_b photon absorption rate due to the actual background light;
- e electron charge;
- I_b/e contribution of the APD bulk leakage current to the APD output;
- M_e modulation extinction ratio of the laser diode output power.

Note that the background light is not considered in a fiber network, i.e., $\lambda_b = 0$ in a fiber network. Thus, background light is not considered in this paper.

In the following, we analyze error-rate performance of turbo-coded optical PPM CDMA systems. First, we present upper bound on BER of M-ary PPM CDMA systems [22]. In the proposed system we assume each user to be assigned unique optical orthogonal code sequence with out-of-phase auto and cross correlations bounded by 1. The probability that a user causes an interference on the ith slot of the desired user is given by

$$P_i(1) = \frac{K^2}{MF}. \tag{12}$$

The conditional probability that a user causes an interference on the jth slot of the desired user given that the user causes an interference on the ith slot $(i \neq j)$ is given by

$$P_{j\,|\,i}(1\,|\,1) = \frac{|i-j|}{M^2}. \tag{13}$$

Thus, the probability that a user causes an interference both on the ith and jth slots $(i \neq j)$ of the desired user is given by

$$P_{i,j}(1,1) = \frac{|i-j|}{M^2} \cdot \frac{K^2}{MF}. \tag{14}$$

Also, the probability that a user causes an interference not on the ith but on the jth slots $(i \neq j)$ of the desired user or vice versa is given by

$$P_{i,j}(1,0) = P_{i,j}(0,1) = \left(1 - \frac{|i-j|}{M^2}\right) \cdot \frac{K^2}{MF}. \tag{15}$$

Thus, the probability that a user causes an interference neither on ith nor jth slot $(i \neq j)$ is given by

$$P_{i,j}(0,0) = 1 - P_{i,j}(1,1) - P_{i,j}(0,1) - P_{i,j}(1,0). \tag{16}$$

We denote the number of users causing an interference on the ith slot by κ_i. Then, the combinatorial probability density function of two variables, κ_i and $\kappa_j, (i \neq j)$, is given by

$$\begin{aligned}\Pr\{\kappa_i = l_i, \kappa_j = l_j\} &= \sum_{r=\max\{0, l_i+l_j-(N-1)\}}^{\min\{l_i,l_j\}} \\ &\times \frac{(N-1)!}{r!(l_i-r)!(l_j-r)!(N-1-l_i-l_j+r)!} \\ &\cdot P_{i,j}(1,1)^r P_{i,j}(1,0)^{l_i-r} P_{i,j}(0,1)^{l_j-r} \\ &\cdot P_{i,j}(0,0)^{N-1-l_i-l_j+r}, \\ & \qquad i, l_j \in \{0,1,\ldots,N-1\}. \end{aligned} \tag{17}$$

We denote output of an APD on the ith slot $(i \in \{0,1,\ldots,M-1\})$ by Y_i. Under assumption of equiprobable inputs, a word-error probability P_e is represented as

$$P_e = \sum_{i=0}^{M-1} P[e\,|\,i] \Pr\{i\} \tag{18}$$

where $\Pr\{i\} = 1/M$ represents an occurrence probability of the ith data. Using a union bound, the conditional word-error probability $P[e\,|\,i]$ is derived as

$$\begin{aligned} P[e\,|\,i] &= \Pr\{Y_j \geq Y_i, \text{some } j \neq i \,|\, i\} \\ &\leq \sum_{j=0, j\neq i}^{M-1} \Pr\{Y_j \geq Y_i \,|\, i\}. \end{aligned} \tag{19}$$

Denoting by P_e^U a union bound on the word-error probability P_e of uncoded optical PPM CDMA systems, P_e^U is represented by

$$\begin{aligned} P_e^U &= \sum_{i=0}^{M-1} \sum_{j=0, j\neq i}^{M-1} \Pr\{Y_j \geq Y_i \,|\, i\} \Pr\{i\} \\ &= \frac{2}{M} \sum_{m=1}^{M-1} (M-m) \Pr\{Y_j \geq Y_i \,|\, i, |i-j| = m\} \\ &= \frac{2}{M} \sum_{m=1}^{M-1} (M-m) \Pr\{Y_m \geq Y_0 \,|\, 0\}. \end{aligned} \tag{20}$$

Here, we rewrite the probability $\Pr\{Y_m \geq Y_0 \,|\, 0\}$ in (20) as follows:

$$\begin{aligned} &\Pr\{Y_m \geq Y_0 \,|\, 0\} \\ &= \sum_{l_0=0}^{N-1} \sum_{l_m=0}^{N-1} \Pr\{Y_m \geq Y_0 \,|\, 0, \kappa_0 = l_0, \kappa_m = l_m\} \\ &\quad \cdot \Pr\{\kappa_0 = l_0, \kappa_m = l_m \,|\, 0\} \qquad (21) \\ &= \sum_{l_0=0}^{N-1} \sum_{l_m=0}^{N-1} \Pr\{Y_m \geq Y_0 \,|\, 0, \kappa_0 = l_0, \kappa_m = l_m\} \\ &\quad \cdot \Pr\{\kappa_0 = l_0, \kappa_m = l_m\}. \qquad (22) \end{aligned}$$

Also, the upper bound on the conditional probability in (21) is given by

$$\begin{aligned} &\Pr\{Y_m \geq Y_0 \,|\, 0, \kappa_0 = l_0, \kappa_m = l_m\} \\ &\quad \leq \Pr\{Y_m \geq Y_0 \,|\, 0, \kappa_0 = 0, \kappa_m = l_m\}. \end{aligned} \tag{23}$$

Substituting (23) into (21), we can have the following equation:

$$\begin{aligned} &\Pr\{Y_m \geq Y_0 \,|\, 0\} \\ &\quad \leq \sum_{l_m=0}^{N-1} \Pr\{Y_m \geq Y_0 \,|\, 0, \kappa_0 = 0, \kappa_m = l_m\} \\ &\quad \cdot \Pr\{\kappa_m = l_m\}. \end{aligned} \tag{24}$$

Substituting (24) into (20), upper bound on P_e^U is given by

$$\begin{aligned} P_e^U &\leq (M-1) \sum_{l_m=0}^{N-1} \binom{N-1}{l_m} \left(\frac{K^2}{MF}\right)^{l_m} \\ &\quad \cdot \left(1 - \frac{K^2}{MF}\right)^{N-1-l_m} \\ &\quad \cdot \Pr\{Y_m \geq Y_0 \,|\, 0, \kappa_0 = 0, \kappa_m = l_m\}. \end{aligned} \tag{25}$$

Denote by $p(d\,|\,i)$ the conditional probability of producing a codeword fragment with output weight d given a randomly selected input sequence of weight i. Following [8], $p(d\,|\,i)$ can be written as

$$p(d\,|\,i) = \frac{t(N_I, i, d)}{\sum_{d'} t(N_I, i, d')} = \frac{t(N_I, i, d)}{\binom{N_I}{i}}. \tag{26}$$

When the random interleaver, that is, the random permutation is selected, the probability $\tilde{p}(i, d_1, d_2\,|\,i)$ that any input sequence $\mathbf{u}$ of weight i will be mapped into codeword fragments of weights d_0, d_1, and d_2 is given by

$$\tilde{p}(d_0, d_1, d_2\,|\,i) = p_1(d_0\,|\,i)p_{7/5}(d_1\,|\,i)p_{7/5}(d_2\,|\,i) \tag{27}$$

for the $(1, 7/5, 7/5)$ code and

$$\tilde{p}(d_0, d_1, d_2\,|\,i) = p_1(d_0\,|\,i)p_{5/7}(d_1\,|\,i)p_{5/7}(d_2\,|\,i) \tag{28}$$

for the $(1, 5/7, 5/7)$ code. To apply the transfer function bounding technique for turbo codes directly to optical PPM CDMA systems, we focus on BPPM, as in [12]. The codeword-error probability P_e is upper bounded as follows:

$$\begin{aligned} P_e &= \sum_{i=1}^{N_I} \Pr[\text{error event of weight } i] \\ &\le \sum_{i=1}^{N_I} \sum_{d_1=0}^{N_I} \sum_{d_2=0}^{N_I} \binom{N_I}{i} \tilde{p}(d_0, d_1, d_2\,|\,i) \\ &\quad \cdot \sum_{\mathbf{l}} \binom{N-1}{l_1}\binom{N-1}{l_2}\cdots\binom{N-1}{l_d} \\ &\quad \cdot \left(\frac{K^2}{2F}\right)^{g(\mathbf{l})} \left(1 - \frac{K^2}{2F}\right)^{d(N-1)-g(\mathbf{l})} \\ &\quad \cdot \Pr\{Y_1 \ge Y_0\,|\,0, \kappa_{\mathbf{0}} = \mathbf{0}, \kappa_{\mathbf{1}} = \mathbf{l}\} \end{aligned} \tag{29}$$

where $\mathbf{0} = (0, 0, \ldots, 0)$, $\mathbf{l} = (l_1, l_2, \ldots, l_d)$, $d = i + d_1 + d_2$, and

$$g(\mathbf{l}) = \sum_{i=1}^{d} l_i. \tag{30}$$

Similarly, the information bit-error probability P_b is upper bounded by

$$\begin{aligned} P_b &= \sum_{i=1}^{N_I} \frac{i}{N_I} \Pr[\text{error event of weight } i] \\ &\le \sum_{i=1}^{N_I} \frac{i}{N_I} \sum_{d_1=0}^{N_I} \sum_{d_2=0}^{N_I} \binom{N_I}{i} \tilde{p}(d_0, d_1, d_2\,|\,i) \\ &\quad \cdot \sum_{\mathbf{l}} \binom{N-1}{l_1}\binom{N-1}{l_2}\cdots\binom{N-1}{l_d} \\ &\quad \cdot \left(\frac{K^2}{2F}\right)^{g(\mathbf{l})} \left(1 - \frac{K^2}{2F}\right)^{d(N-1)-g(\mathbf{l})} \\ &\quad \cdot \Pr\{Y_1 \ge Y_0\,|\,0, \kappa_{\mathbf{0}} = \mathbf{0}, \kappa_{\mathbf{1}} = \mathbf{l}\}. \end{aligned} \tag{31}$$

The receiver integrates the APD output over the last chip interval T_c. The accumulated output during each chip interval is assumed to be a Gaussian random variable [20], [21]. Over the last chip K marks at λ_s incident photon arrival rate are summed up. In addition bulk leakage current, surface leakage current, and thermal noise are added over the last chip. The conditional probability $\Pr\{Y_1 \ge Y_0\,|\,0, \kappa_{\mathbf{0}} = \mathbf{0}, \kappa_{\mathbf{1}} = \mathbf{l}\}$ is derived as follows:

$$\begin{aligned} &\Pr\{Y_1 \ge Y_0\,|\,0, \kappa_{\mathbf{0}} = \mathbf{0}, \kappa_{\mathbf{1}} = \mathbf{l}\} \\ &\quad = \int_{-\infty}^{\infty} \frac{1}{\sqrt{2\pi\sigma_d^2}} e^{-(x-\mu_1)^2/2\sigma_1^2} \\ &\qquad \cdot \int_{-\infty}^{x} \frac{1}{\sqrt{2\pi\sigma_0^2}} e^{-(y-\mu_0)^2/2\sigma_0^2}\, dy\, dx. \end{aligned} \tag{32}$$

Here, the means, μ_0 and μ_1, and the variances, σ_0^2 and σ_1^2 of Y_0 and Y_1, are derived, respectively, as follows:

$$\begin{aligned} \mu_0 &= d\{GT_c[K\lambda_s + (KN-K)\lambda_s/M_e + K \\ &\qquad + I_b/e] + T_c I_s/e\}, \end{aligned} \tag{33}$$

$$\begin{aligned} \mu_1 &= GT_c[g(\mathbf{l})\lambda_s + (dKN - g(\mathbf{l}))\lambda_s/M_e + dK\lambda_b \\ &\qquad + dI_b/e] + dT_c I_s/e, \end{aligned} \tag{34}$$

$$\begin{aligned} \sigma_0^2 &= d\{G^2 F_e T_c[K\lambda_s + (KN-K)\lambda_s/M_e + K\lambda_b \\ &\qquad + I_b/e] + T_c I_s/e + \sigma_{\text{th}}^2\}, \end{aligned} \tag{35}$$

$$\begin{aligned} \sigma_1^2 &= G^2 F_e T_c[g(\mathbf{l})\lambda_s + (dKN - g(\mathbf{l}))\lambda_s/M_e + dK\lambda_b \\ &\qquad + dI_b/e] + dT_c I_s/e + d\sigma_{\text{th}}^2. \end{aligned} \tag{36}$$

Here, G is the average APD gain, I_b is the bulk leakage current, I_s is the APD surface leakage current, F_e is the excess noise factor given by

$$F_e = k_{\text{eff}} G + (2 - 1/G)(1 - k_{\text{eff}}) \tag{37}$$

where k_{eff} is the APD effective ionization ratio, and σ_{th}^2 is the variance of thermal noise written as

$$\sigma_{\text{th}}^2 = 2k_B T_r T_c/(e^2 R_L) \tag{38}$$

where

- k_B Boltzmann's constant;
- T_r receiver noise temperature;
- R_L receiver load resistor.

Note that the word- and bit-error probabilities P_e and P_b bounded in (29) and (31) are averages over a randomly chosen permutation π [8].

IV. Numerical Results

We use typical APD parameters in Table I in the numerical calculation to be presented in this section.

Note that P_W denotes the unit received laser power in a delay-line of optical correlator. Numerical calculation for performance of turbo-coded optical PPM CDMA systems with long interleaver length is not feasible. Thus, we focus on the system with short interleaver length, N_I=31. Note that

TABLE I
LINK PARAMETERS

Name	Symbol	Value
Laser wavelength		1.55 μm
APD quantum efficiency	η	0.6
APD gain	G	100
APD effective ionization ratio	k_{eff}	0.02
APD bulk leakage current	I_b	0.1 nA
APD surface leakage current	I_s	10 nA
Modulation extinction ratio	M_e	100
Receiver noise temperature	T_r	1100°K
Receiver load resistor	R_L	1030 Ω

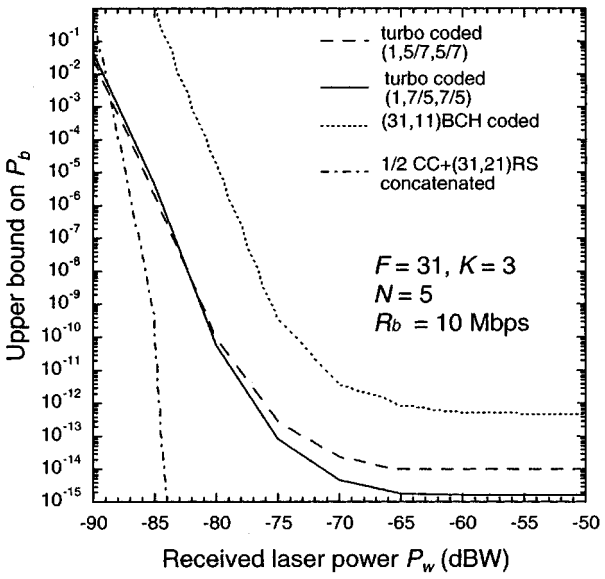

Fig. 7. Bounds on P_b versus received laser power P_W where the bit rate $R_b = 10$ Mb/s, the interleaver length $N_I = 31$, the number of simultaneous users $N = 5$, and OOC with $F = 31$ and $K = 3$.

the bound on BER is applicable where the optical CDMA is usually operated.

Figs. 7 and 8 show upper bounds on the bit-error probability versus received laser power P_W where the interleaver length $N_I = 31$, the number of simultaneous users $N = 5$, OOC with $F = 31$ and $K = 3$ for turbo-coded optical PPM CDMA systems and $(31, 11)$ BCH-coded optical PPM CDMA system where we use optimum soft-decision decoding of BCH codes [13], [14]. Bit rates are $R_b = 10$ Mb/s and 100 Mb/s in Figs. 7 and 8, respectively. Note that bit and chip rates are approximately the same for all the systems. Note also that when the

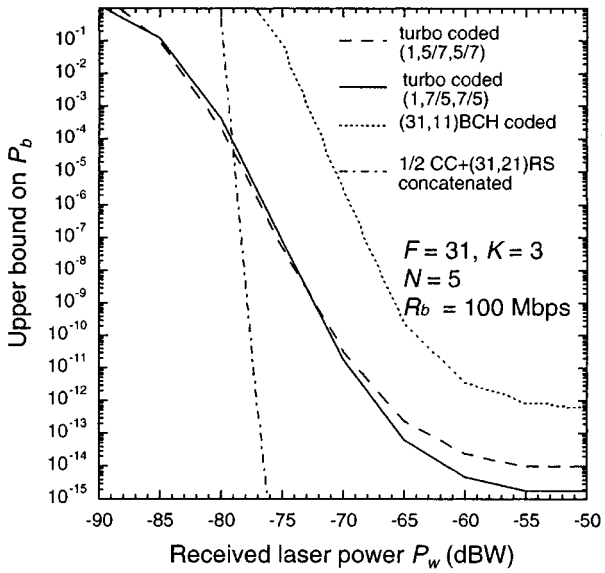

Fig. 8. Bounds on P_b versus received laser power P_W where the bit rate $R_b = 10$ Mb/s, the interleaver length $N_I = 31$, the number of simultaneous users $N = 5$, and OOC with $F = 31$ and $K = 3$.

number of simultaneous users is larger than the code weight, i.e., $N > K$, an error floor exists in the performance of uncoded PPM CDMA systems. We can see that among three systems, concatenated coding system has the best performance when the received laser power is not small. This is because turbo codes need larger block length (interleaver size) to achieve good performance, and also because turbo codes have good performance particularly when the received laser power is small. We can see that turbo-coded optical PPM CDMA systems have better BER performance than BCH-coded optical CDMA systems. We can also see that both $(1, 7/5, 7/5)$ and $(1, 5/7, 5/7)$ turbo codes can achieve about the same performance. As shown for optical PPM systems [12], no abrupt transition can be seen for the transfer function bound for turbo-coded optical PPM CDMA systems.

Figs. 9 and 10 show upper bounds on the bit-error probability versus the number of users N where the interleaver length $N_I = 31$, the received laser power is $P_W = -80$ dBW in Fig. 9 and $P_W = -75$ dBW in Fig. 10, respectively. As a code sequence, we use OOC with $F = 31$ and $K = 3$ for turbo-coded optical PPM CDMA systems and BCH-coded optical PPM CDMA system where we use optimum soft-decision decoding of BCH codes [13], [14]. Bit rates are $R_b = 10$ Mb/s and 100 Mb/s in Figs. 6 and 7, respectively. Note that the bit and chip rates are approximately the same for all the systems. Note also that the uncoded optical PPM CDMA systems cannot accommodate more users than the value of weight of the code sequence used in the system, even with large received laser power. Note also that when the received laser power is as mentioned above, the performance of concatenated systems is out of region of the figures and not shown in the figures. However, when the received laser power is smaller than the values mentioned above, turbo-coded systems have better performance. We can see that turbo-coded optical PPM CDMA systems have better BER performance than BCH-coded optical PPM CDMA systems in both cases. We can also see that the performance difference between

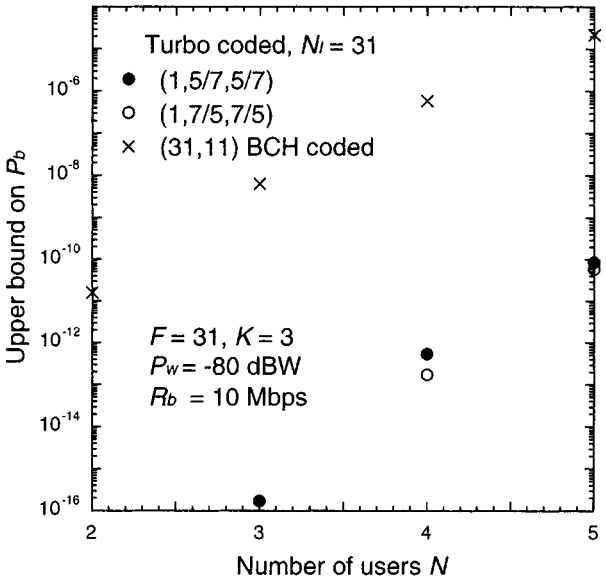

Fig. 9. Bounds on P_b versus the number of users N where the received laser power $P_W = -80$ dBW, the bit rate $R_b = 10$ Mb/s, the interleaver length $N_I = 15$, and OOC with $F = 31$ and $K = 3$.

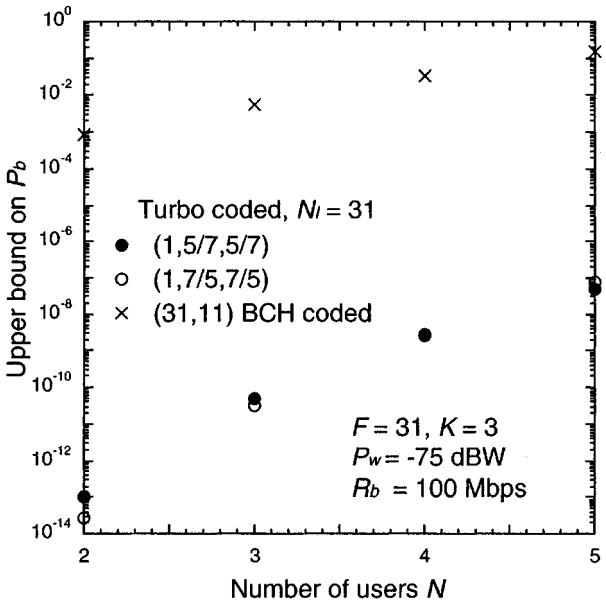

Fig. 10. Bounds on P_b versus the number of users N where the received laser power $P_W = -75$ dBW, the bit rate $R_b = 100$ Mb/s, the interleaver length $N_I = 15$, and OOC with $F = 31$ and $K = 3$.

$(1, 7/5, 7/5)$ and $(1, 5/7, 5/7)$ turbo codes becomes smaller as the number of users is increased. Thus, we can accommodate many users in optical CDMA networks by using turbo codes.

V. Conclusion

We have obtained the upper bounds on the BER for turbo-coded optical PPM CDMA systems. The bounds were derived using transfer function bounding techniques. We applied the techniques to the PCCC schemes. We showed that turbo-coded systems have better BER performance than BCH-coded systems and thus can accommodate more users. We also showed that concatenated systems have better performance than turbo-coded systems when the block length is small and the received laser power is somewhat large.

References

[1] J. A. Salehi, "Code division multiple-access techniques in optical fiber networks—Part I: Fundamental principles," *IEEE Trans. Commun.*, vol. 37, pp. 824–833, Aug. 1989.

[2] J. A. Salehi and C. A. Brackett, "Code division multiple-access techniques in optical fiber networks—Part II: Systems performance analysis," *IEEE Trans. Commun.*, vol. 37, pp. 834–842, Aug. 1989.

[3] T. Ohtsuki, I. Sasase, and S. Mori, "Effects of hard-limiter and error correction coding on performance of direct-detection optical CDMA systems with PPM signaling," *IEICE Trans. Fundamentals*, vol. E78-A, pp. 1092–1101, Sept. 1995.

[4] J.-H. Wu and J. Wu, "Synchronous fiber-optic CDMA using hard-limiter and BCH codes," *J. Lightwave Technol.*, vol. 13, pp. 1169–1176, June 1995.

[5] T. Ohtsuki, "Channel interference cancellation using electrooptic switch and optical hard-limiters for direct-detection optical CDMA systems," *J. Lightwave Technol.*, vol. 16, pp. 520–526, Apr. 1998.

[6] H. M. H. Shalaby, "Chip-level detection in optical code division multiple access," *J. Lightwave Technol.*, vol. 16, pp. 1077–1087, June 1998.

[7] C. Berrou, A. Glavieux, and P. Thitimajshima, "Near shanon limit error correcting coding and decoding: Turbo-codes (1)," in *Proc. ICC'93*, Geneva, Switzerland, May 1993, pp. 1064–1070.

[8] D. Divsalar, S. Dolinar, and F. Pollara, "Transfer Function Bounds on the Performance of Turbo Code," Jet Propulsion Lab., Pasadena, CA, TDA Pogr. Rep. 42-122, Aug. 1995.

[9] S. Benedetto and G. Montorsi, "Unveiling turbo codes: Some results on parallel concatenated coding schemes," *IEEE Trans. Inform. Theory*, vol. 42, pp. 409–428, Mar. 1996.

[10] ——, "Design of parallel concatenated convolutional codes," *IEEE Trans. Commun.*, vol. 44, pp. 591–600, May 1996.

[11] D. Divsalar and F. Pollara, "Turbo-codes for PCS applications," in *Proc. ICC'95*, Seattle, WA, June 1995, pp. 54–59.

[12] K. Kiasaleh, "Turbo-coded optical PPM communication systems," *J. Lightwave Technol.*, vol. 16, pp. 18–26, Jan. 1998.

[13] J. G. Proakis, *Digital Communications*, 3rd ed. New York: McGraw-Hill, 1995.

[14] T. Ohtsuki, T. Kaneko, and J. M. Kahn, Performance analysis of linear binary block coded optical PPM CDMA systems with soft-decision decoding, in 2000 IEEE Global Telecommunications Conf.. submitted.

[15] F. R. K. Chung, J. A. Salehi, and V. K. Wei, "Optical orthogonal codes: Design, analysis, and applications," *IEEE Trans. Inform. Theory*, vol. 35, pp. 595–604, May 1989.

[16] D. Divsalar and F. Pollara, "Turbo Codes for Deep-Space Communications," Jet Propulsion Lab., Pasadena, CA, TDA Pogr. Rep. 42-120, Feb. 1995.

[17] L. C. Perez, J. Seghers, and D. J. Costello Jr., "A distance spectrum interpretation of turbo codes," *IEEE Trans. Inform. Theory*, vol. 42, pp. 1698–1709, Nov. 1996.

[18] P. Robertson, "Illuminating the structure of parallel concatenated recursive systematic (TURBO) codes," in *Proc. GLOBECOM'94*, San Francisco, CA, Nov. 1994, pp. 1298–1303.

[19] S. Kim, M. Kang, S. Park, Y. Choi, and S. Han, "Incoherent bidirectional fiber-optic code-division multiple access networks," *IEEE Photon. Technol. Lett.*, vol. 12, pp. 921–923, July 2000.

[20] H. M. Kwon, "Optical orthogonal code-division multiple access system—Part I: APD noise and thermal noise," *IEEE Trans. Commun.*, vol. 42, pp. 2470–2479, July 1994.

[21] J. B. Abshire, "Performance of OOK and low-order PPM modulations in optical communications when using APD-based receivers," *IEEE Trans. Commun.*, vol. COM-32, pp. 1140–1143, Oct. 1984.

[22] H. M. H. Shalaby, "A comparison between the performance of number-state and coherent-state optical CDMA in lossy photon channels," *IEEE J. Select. Areas Commun.*, vol. 13, pp. 592–602, Apr. 1995.

Tomoaki Ohtsuki (S'91–M'95) received the B.E., M.E., and Ph.D. degrees in electrical engineering from Keio University, Yokohama, Japan, in 1990, 1992, and 1994, respectively.

From 1994 to 1995, he was a Post Doctoral Fellow and a Visiting Researcher of Electrical Engineering at Keio University. From 1993 to 1995, he was a Special Researcher of Fellowships of the Japan Society for the Promotion of Science for Japanese Junior Scientists. From 1995 to 1999, he was an Assistant Professor of Science University of Tokyo. Since 2000, he has been a Lecturer (tenured) of the Science University of Tokyo. Since 1997, he has been a Research Fellow of Sinkawasaki Research Center, Telecommunication Advancement Organization of Japan. Since 1998, he has also been a Visiting Researcher of Keio University. From 1998 to 1999, he was with the Department of Electrical Engineering and Computer Sciences, University of California, Berkeley. He is engaged in research on optical communication systems, wireless communication systems, and information theory.

Dr. Ohtsuki is a recipient of the 1997 Inoue Research Award for Young Scientists, the 1997 Hiroshi Ando Memorial Young Engineering Award, and Erricson Young Scientist Award 2000. He is a Member of IEICE and the Society of Information Theory and Its Applications.

Joseph M. Kahn (M'90–SM'98–F'00) received the A.B., M.A., and Ph.D. degrees in physics from University of California, Berkeley, in 1981, 1983, and 1986, respectively. His doctoral research involved infrared spectroscopy of hydrogen-related impurity complexes in semiconductors.

Currently, he is a Professor and Vice Chair for Graduate Matters in the Department of Electrical Engineering and Computer Sciences, the University of California. From 1987 to 1990, he was a Member of Technical Staff in the Lightwave Communications Research Department of AT&T Bell Laboratories, where he performed research on multi-gigabit-per-second coherent optical fiber transmission systems and related technologies, setting several world records for receiver sensitivity. He joined the faculty of the University of California in 1990. His current research addresses several areas of communications, including wireless communication using antenna arrays, wireless communication for micro-electromechanical systems (MEMS), optical wireless communication, and optical fiber communications. He has authored or coauthored about 120 technical papers, and has presented more than 20 invited talks at major conferences. At the University of California, he has been principal supervisor of eight doctoral theses, including D. Shiu's dissertation "Wireless Communication using Dual Antenna Arrays", which won the Sakrison Prize . Among these eight former doctoral students, three are currently faculty members at major research universities.

Dr. Kahn won a Best Paper Award at the ACM/IEEE Mobicom'99 Conference for his paper "Mobile Networking for Smart Dust" which he coauthored with K. S. J. Pister. He also received the National Science Foundation Presidential Young Investigator Award in 1991. He is a Fellow of the IEEE, and a member of the IEEE Communications Society, the IEEE Information Theory Society, and the IEEE Lasers and Electro-Optics Society. He is serving currently as a Technical Editor of *IEEE Personal Communications Magazine*.